DEUTSCHES ELEKTRONEN-SYNCHROTRON DESY

DESY 90-072
PHE 90-08
June 1990

Structure Functions, Parton Distributions and QCD Tests at HERA

J. Blümlein

Institut für Hochenergiephysik der Akademie der Wissenschaften, Zeuthen

G. A. Schuler

II. Institut für Theoretische Physik, Universität Hamburg

ISSN 0418-9833

NOTKESTRASSE 85 · 2 HAMBURG 52

To be sure that your preprints are promptly included in the
HIGH ENERGY PHYSICS INDEX ,
send them to the following address (if possible by air mail) :

DESY
Bibliothek
Notkestrasse 85
2 Hamburg 52
Germany

DESY 90-072
PHE 90-08
June 1990

STRUCTUREFUNCTIONS, PARTONDISTRIBUTIONS AND QCD-TESTS AT HERA +)

JOHANNES BLUEMLEIN
Institute for High Energy Physics, Academy of Sciences
Platanenallee 6, Zeuthen, 1615, GDR

and

GERHARD A. SCHULER
II. Institute for Theoretical Physics
University of Hamburg
Luruper Chaussee 149, D-2000 Hamburg 50, FRG

ABSTRACT

The possibilities are reviewed to measure the structure functions and quark and gluon distributions in the HERA energy range. Conditions are discussed to measure Λ_{QCD} and $\alpha_s(Q^2)$ from the scaling violations of structure functions.

1. Introduction

In early 1991 two experiments ZEUS an H1 [1] will be set into operation at the ep-collider HERA [2]. One of the main subjects to be studied by these experiments is the

measurement of the proton structurefunctions, parton-distributions and the scaling violations of these quantities. HERA will operate at a cms energy $s = 4 \cdot E_e \cdot E_p = 4 \times 30 \times 820$ GeV^2 and a nominal luminosity $L = 1.5 \cdot 10^{31}$ cm^{-2} sec^{-1}. The kinematical range which has been explored by lepton-nucleon scattering experiments so far [3] $1 < Q^2 < 300$ GeV^2 and $0.01 < x < 0.9$ can be extended by roughly two orders of magnitude both in x and Q^2 by these experiments.

A precise measurement of the structurefunction $F_2(x,Q^2)$ will be possible down to very low x ($x \sim 10^{-4}$) and up to $Q^2 \sim O(10^4 \text{GeV})$, which allows to test QCD in new kinematical ranges [4,5]. Particularly, it will be interesting to investigate the low-x range of F_2 since yet untested QCD contributions [6-8] could influence its x- and Q^2-dependence in this range. At high Q^2 different possibilities exist to combine $e^{\pm}p$-neutral and charged current cross sections to unfold individual quark distributions and combinations of them [9,10]. Further, the gluon distribution can be determined using different quantities as $R = \sigma_L/\sigma_T$ [11], J/ψ - [12] and open charm production [13] and the singlet component in QCD-fits [4] of F_2.

The measurement of all these quantities presumes detailed investigations of a series of systematic effects and theoretical conditions as the smearing functions, the calibration uncertainties of the calorimeters, the

electroweak radiative corrections and further theoretical corrections in some of the measurements. Due to the size of these effects only a limited part of the available phase space can be used for the measurement of the structure functions. Because most of the issues which we will discuss are rather dependent on these conditions they will be discussed in section 2 briefly. In section 3 possible measurements of structure functions are considered. Different ways to unfold quark distributions from the deep inelastic scattering cross sections are discussed in section 4. Estimates on the potential of HERA to measure Λ_{QCD} and $\alpha_s(Q^2)$ including estimates on systematic effects are given in section 5. In section 6 a survey on different possibilities to determine the gluon distribution at HERA is given and section 7 contains the conclusions.

2. Systematic Effects and Theoretical Corrections

2.1. Smearing Corrections and Systematic Effects

These effects have been considered in detail in ref. [14] both for the measurement of the final state electron and the current jet. Due to the finite resolution of the detectors one has to account for smearing and systematic effects to derive the structurefunctions from measured event distributions. The dominant contributions due to the

smearing functions are implied by the resolutions of both the electromagnetic and hadronic calorimeters. They are given by $\delta E_h/E_h = 0.35 \ldots 1.0/E_h^{1/2} + 0.02$ and $\delta E_e/E_e = 0.13 \ldots 0.17/E_e^{1/2}$. Further, one has to consider the precision of the absolute calibration of the energy measurement also, for which 1 % for the electron measurement and 2 % for the jet measurement might be obtained. Using a Monte Carlo calculation contours in x and Q^2 were derived in [14]. They are depicted in fig.1 for the cms energy $\sqrt{s}$ = 314 GeV and a possible low energy option at HERA with E_e = 15 GeV and E_p = 300 GeV, $\sqrt{s}$ = 134 GeV [15].

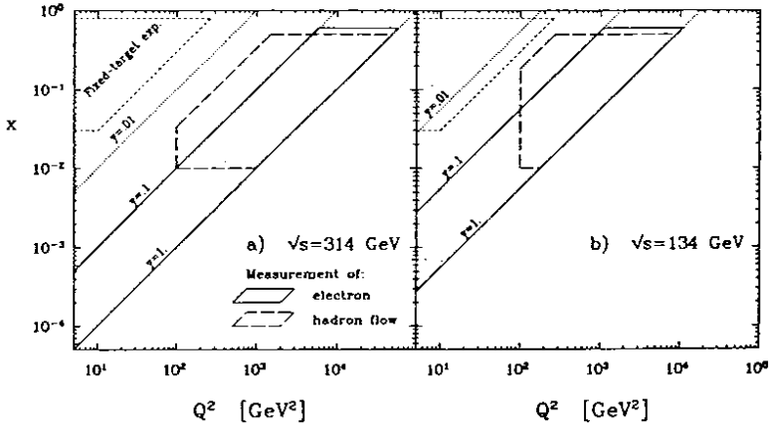

Fig. 1 Kinematical ranges

The electron measurement is bounded by 0.1 < y but ranges to very low x. Due to trigger conditions the hadron-flow measurement is bounded by 100 $GeV^2 < Q^2$ but the resolution

allows to measure down to $y \sim 0.03$. Comparing this range, which we will refer to as the accessible kinematical range at HERA subsequently, with the kinematical range explored so far one observes a gap of about one order of magnitude in Q^2 for the nominal HERA energy. This could be narrowed by measuring the structure functions at lower energies (see fig.1b) and/or seeking for a further improvement of the resolution at low y. Note, that the closest contact to the kinematical range of the fixed target experiments comes from the range of jet measurement in both cases.

Among the systematic effects the calibration uncertainty of the calorimeters is one of the important contributions. Because this effect is particularly large e.g. in the case of the measurement of Λ_{QCD} [5] we discuss it in more detail here.

A shift in the measured electron or hadronic energy $\delta E_{e,H}/E_{e,H} = \pm \varepsilon_{e,H}$ will induce a systematic shift in the kinematical variables x,y and Q^2 which are given for $\varepsilon_{e,H} \ll 1$ by

$$\hat{x}/x \sim 1+\varepsilon_e/y \qquad \hat{x}/x \sim 1+\varepsilon_H/(1-y) \qquad (1a)$$

$$\hat{y}/y \sim 1+\varepsilon_e-\varepsilon_e/y \qquad \hat{y}/y \sim 1+\varepsilon_H \qquad (1b)$$

$$\hat{Q}^2/Q^2 \sim 1+\varepsilon_e \qquad \hat{Q}^2/Q^2 \sim 1+\varepsilon_H(2-y)/(1-y) \qquad (1c)$$

From these relations it follows, that one can get a nearly

unperturbed Q^2 measurement from the final state electron and a nearly unperturbed y measurement from the final state hadrons as long as $\varepsilon_{e,H}$ are small. Otherwise the x and y (or x and Q^2) measurements fail at low (high) y for the electron (hadron) measurement due to the finite miscalibration. Note, that the relations (1) are derived using the kinematics of the Born process only. Modified results would be obtained for the $O(\alpha)$ photon Bremsstrahlung contributions.

2.2. Radiative Corrections

The electroweak radiative corrections to the inclusive neutral and charged current cross sections are the major theoretical corrections which have to be considered for the extraction of structure functions in the HERA energy range. They have been calculated by different groups during the last years [16-21] in complete [16,17,20] and leading log calculations [18,19,21]. Recently, numerical agreement has been obtained among all approaches at the per cent level. Because of the high value of $s \sim 10^5$ GeV^2 both the corrections to the neutral and charged current cross section are widely dominated by the QED-corrections, even by their leading log contributions. This was demonstrated in [18,19] for the neutral current and in [19] for the charged current reactions. A comparison for the relative correction $\delta_i =$

$d^2\sigma(O(\alpha))/d^2\sigma_0$ to neutral and charged current e^- p-scattering for the complete [17] and approximate calculation [19] is given in fig. 2 defining the variables x and y at the leptonic vertex.

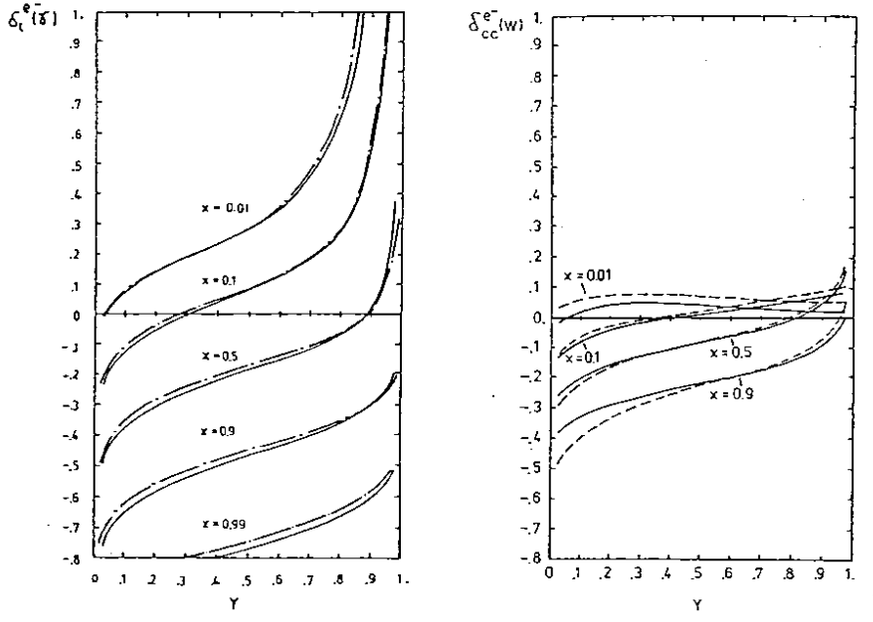

Fig. 2: Comparison of the radiative corrections to deep inelastic neutral and charged current e^- p-reactions. Full lines: leading log approximation [19]; -·-·and --- line: complete calculations [17].

The neutral current radiative corrections become rather large at low x and high y while in the case of charged current reactions the corrections are of O(10%) in this range. At low y soft photon bremsstrahlung causes large negative corrections.

As outlined in sect. 2.1 in wide ranges of x and Q^2

the kinematical variables can only be determined via the jet measurement. It is shown in [21] that the radiative corrections can be calculated analytically for this case and yield new y-dependent factors in front of the structure functions of the Born cross sections. The corrections are shown in fig. 3 for different values in x in the leading log approximation.

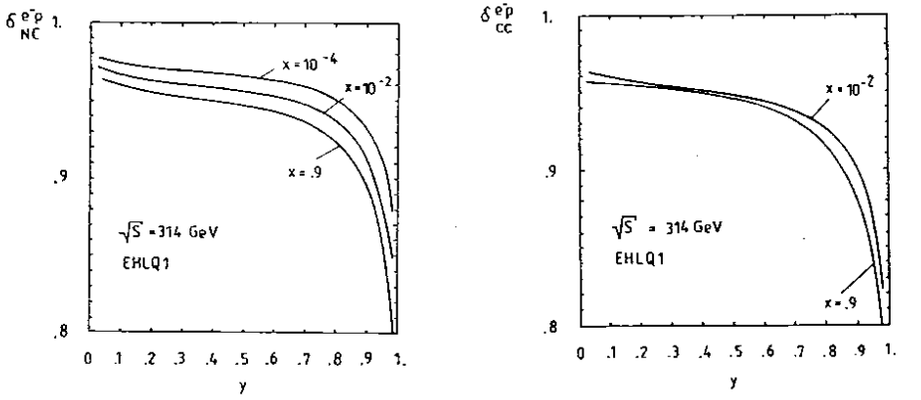

Fig. 3: Radiative corrections to deep inelastic neutral and charged current $e^{\bullet}p$ reactions. The kinematical variables are defined from jet measurement [21].

The variation in x is only logarithmic and the corrections are rather small compared to the case discussed before. At high y a large negative contribution is caused due to soft photon emission. Since there is a range in which both the electron and jet measurement can be used to measure the kinematical variables the inclusive radiative corrections can be also controlled experimentally. Subsequently we will discuss the measurement of structure functions and

parton distributions assuming that the radiative corrections are carried out already and consider the Born cross sections only.

3. Measurement of Structure Functions

The Born cross sections for deep inelastic neutral and charged current reactions are determined by 14 structure functions. They can be written in the form

$$d^2\sigma(e^{\pm}p \to e^{\pm}_{\nu_e} X)/dx\,dQ^2 = \frac{2\pi\alpha^2}{xQ^4}\,\hat{\sigma}^{\pm}_i \qquad (2)$$

with

$$\hat{\sigma}^{\pm}_{NC} = y^2 2x F_1^{\pm}(x,Q^2) + 2(1-y) F_2^{\pm}(x,Q^2) + Y_- x F_3^{\pm}(x,Q^2) \qquad (3)$$

and

$$\hat{\sigma}^{\pm}_{CC} = \frac{1}{2}\kappa_W^2(Q^2)\left[y^2 2x W_1^{\pm} + 2(1-y) W_2^{\pm} \mp Y_- x W_3^{\pm}\right] \qquad (4)$$

for neutral and charged current reactions. In leading order the Callen-Gross relations $2x F_1^{\pm} = F_2^{\pm}$ and $2x W_1^{\pm} = W_2^{\pm}$ hold. The functions $F_i^{\pm}$ are not the generic structure functions but contain also propagator terms. They are given by

$$2x F_1^{\pm} = 2x F_1 - v_e \kappa_Z(Q^2) 2x G_1 + \kappa_Z^2(Q^2)(v_e^2+a_e^2) 2x H_1 \qquad (5a)$$

$$F_2^{\pm} = F_2 - v_e \kappa_Z(Q^2) G_2 + \kappa_Z^2(Q^2)(v_e^2+a_e^2) H_2 \qquad (5b)$$

$$x F_3^{\pm} = \pm a_e \kappa_Z(Q^2) x G_3 \mp \kappa_Z^2(Q^2) 2 v_e a_e x H_3 \qquad (5c)$$

The neutral and charged current structure functions are related to the quarkdistributions by

$$2x(F_1, G_1, H_1) = x\sum_q (Q_q^2, 2Q_q v_q, v_q^2+a_q^2)(q+\bar{q}) \qquad (6a)$$

$$x(G_3, H_3) = 2x\sum_q (Q_q a_q, v_q a_q)(q-\bar{q}) \qquad (6b)$$

$$W_2^{\pm} = 2x\sum_i q_{d(u)} + \bar{q}_{u(d)} \qquad (6c)$$

$$x W_3^{\pm} = 2x\sum_i q_{d(u)} - \bar{q}_{u(d)} \qquad (6d)$$

and $f_2 = 2xf_1 + f_L$, $f_i = F_i, G_i, H_i$, where f_L can be rewritten in terms of the according longitudinal parton densities. Here $Y_- = 1-(1-y)^2$, $\kappa_Z(Q^2) = Q^2/(Q^2+M_Z^2)/4S_\theta^2 C_\theta^2$, $\kappa_W(Q^2) = Q^2/(Q^2+M_W^2)/4S_\theta^2$, and Q_f, $a_f = I_f^3$, $v_f = I_f^3 - 2Q_f \sin^2\theta_W$ are the electroweak couplings.

To illustrate the event rates which can be measured at HERA the integrated event rates for $Q^2 > Q_0^2$ are depicted for the different cross sections, $x > 0.01$, $y > 0.03$ and an integrated luminosity of 100 pb^{-1} in fig. 4. At Q^2 lower than $\sim 10^3$ GeV^2 both neutral current cross sections are nearly identical and nearly no charged current events are found in this range. Thus, the only structure functions which can be measured in this range are F_2 and F_L.

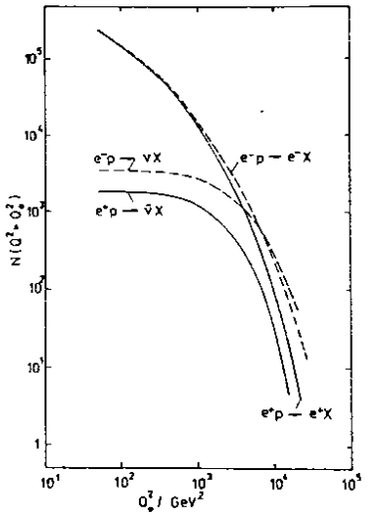

Fig. 4: Neutral and charged current event rates for $Q^2 > Q_0^2$ [9].

The statistical precision which can be obtained for the measurement of F_2 is illustrated in fig. 5. At low x the slopes in $\ln(Q^2)$ are rather large. For $x > 0.01$ at high y the contributions due to the electroweak terms become visible. Due to the smaller statistics in this range F_2 remains to be a good approximation up to rather high Q^2.

For the measurement of the longitudinal structure function F_L the measurement of the neutral current cross section at at least two different beam energies is required to determine F_L from the y dependence in equal (x,Q^2)-bins . Choosing E_p= 820 and E_p= 300 GeV in [9] the precision of $R = F_L / F_2$ was estimated assuming a luminosity of

100 pb^{-1} for each option.

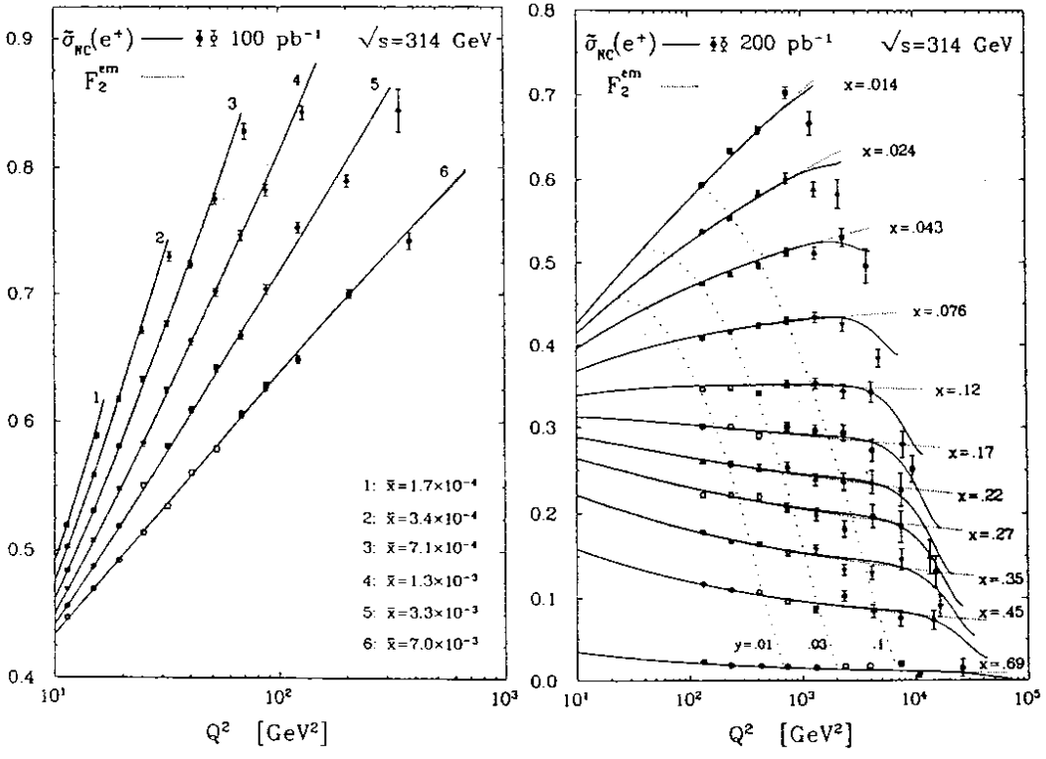

Fig. 5: Statistical precision for F_2

As shwown in fig. 6 R can be precisely measured at $x < 0.01$ which is important for the determination of F_2 and a possibility to measure the gluon distribution at low x [11],cf. sect. 6.

From the difference of the cross sections $\hat{\sigma}^{\pm}_{NC}$ the structure function xG_3 arising in the γ-Z interference

term can be measured.

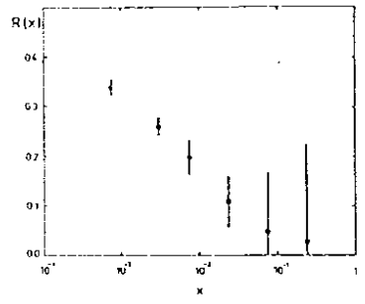

Fig. 6: Statistical precision for a R-measurement using E_p= 820 and E_p= 300 GeV.

For this distribution only the x-shape can be measured with sufficient precision. As seen from fig. 4 , this distribution is only measurable for $Q^2 > 10^3$ GeV^2 . Because it is a valence distribution its Q^2dependence is rather weak only and can not be resolved within the statistical errors.

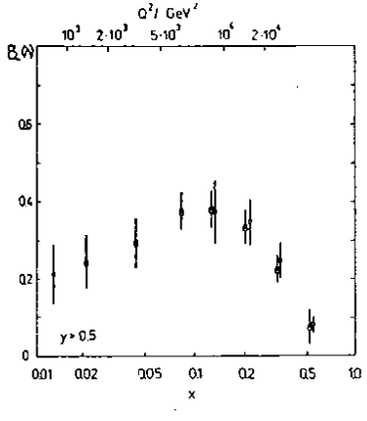

Fig. 7: Determination of xG_3 from $\hat{\sigma}^-_{NC}$ and $\hat{\sigma}^+_{NC}$. The luminosities used are 100 pb^{-1} per beam.

The charged current cross sections contain six different structurefunctions. Even if one assumes the validity of the Callen-Gross relation an unfolding of the structure functions is not possible. However, at low y the Y_- terms become small and both from the cross sections $\hat{\sigma}^+_{CC}$ and $\hat{\sigma}^-_{CC}$ the functions $W_2^{\pm}$ can be determined in an approximate way. This is illustrated in fig. 8 for the structurefunction W_2^- .

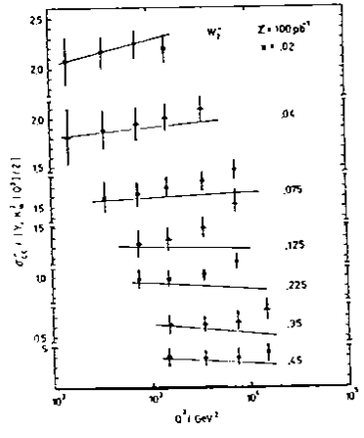

Fig. 8: Determination of W_2^- from $\hat{\sigma}^-_{CC}$ at low y.

4. Unfolding of Quark Distributions

Since four different deep inelastic scattering cross sections can be measured at HERA at most four combinations of quark distributions can be unfolded from the cross

sections. If a suitable basis of those functions is choosen one has to solve the linear problem [9,10]

$$\begin{pmatrix} \hat{\sigma}^{+}_{NC} \\ \hat{\sigma}^{-}_{NC} \\ \hat{\sigma}^{+}_{CC} \\ \hat{\sigma}^{-}_{CC} \end{pmatrix} = (A_{ij}(y,Q^2)) \begin{pmatrix} x q_1 \\ x q_2 \\ x q_3 \\ x q_4 \end{pmatrix} \qquad (7)$$

with $\hat{\sigma}_i = xQ^4 d^2\sigma_i/dxdQ^2/2\pi\alpha^2$

In principle (7) can be solved in the whole available kinematical range but practically one has to guarantee that i) $(A_{ij}(y,Q^2))$ is not degenerate and ii) the errors of $\hat{\sigma}_i$ are sufficiently small to yield a meaningful measurement for the distributions $xq_i(x,Q^2)$. At low Q^2 ($Q^2 < 10^3$ GeV^2) both conditions are not met: because of the dominance of γ-exchange both neutral current cross sections are nearly equal and $(A_{ij}(y,Q^2))$ tends to degenerate. The charged current statistics is rather poor in this range which would induce large errors for xq_i. Thus, this method can be applied best at high $Q^2 \gtrsim O(10^3$ GeV$^2)$ where all $\hat{\sigma}_i$'s are of comparable magnitude. Because the overall statistics both for neutral and charged current events is of a few $10^{3..4}$ only the determination of the x-shapes of the distributions xq_i is possible. However, due to the high Q^2 still differences in shape might be found

comparing with measurements at lower Q^2 in fixed target experiments [10].

Apart from the exact unfolding method (7) one can extract some of the combinations xq_i also approximately in some parts of the kinematical range. This is discussed in ref. [9,10]. An example for this method is the extraction of parton distributions in the valence range $x > 0.25$. The cross sections $\hat{\sigma}^{\pm}_{CC}$ are proportional to xu_v and xd_v in this range resp. From $\hat{\sigma}^{\pm}_{NC}$ one can measure $\frac{4}{9}xu_v + \frac{1}{9}xd_v$ for $Q^2 \lesssim 10^3$ GeV^2. More complicated examples are discussed in ref. [10].

To illustrate the statistical precision of these methods fig. 9 shows possible measurements of the x-shape of $F_s = \sum_i x(q_i + \bar{q}_i)$. The statistics used both for the approximate representation $\hat{\sigma}^{-}_{CC} + \hat{\sigma}^{+}_{CC}/(1-y)^2$ (fig.9a) and the exact unfolding (fig.9b) using the basis $(xu_v, xd_v, x\sum_i u_i + \bar{u}_i, x\sum_i d_i + \bar{d}_i)$ amounts to 400 pb^{-1}.

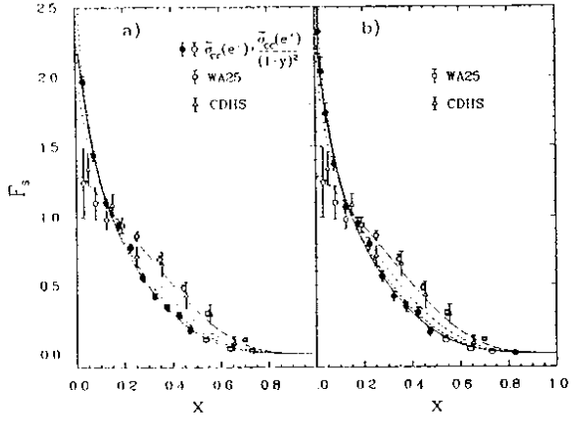

Fig. 9: Possible determination of $F_s(x)$ via an approximate representation and exact unfolding [10]

Although in principle 14 different x-distributions can be determined only 7 can be measured with a sufficient precision. Particularly it will be difficult to measure $x\sum_i d_i$, $x\sum_i \bar{d}_i$, and at lower x also of xd_v [10].

5. QCD Tests

The analysis of the Q^2 dependence of the measured structure functions at constant x allows to determine the QCD scale Λ and $\alpha_s(Q^2)$ [22]. In a systematic analysis [9,5,6] a variety of structure functions and combinations of parton distributions which can be unfolded from the neutral and charged current cross sections was investigated. It turns out that only $F_2(x,Q^2)$ can be measured at a sufficient precision required for a QCD-test.

F_2 can be measured from $\hat{\sigma}^{\pm}_{NC}$ directly at $Q^2 \lesssim O(10^3\,\mathrm{GeV}^2)$. At higher values of Q^2 electroweak terms contribute but also the statistical errors become larger. One can define a cut

$$|1 - \sigma^{\pm}_{NC}/F_2 Y_+|/\delta F_2 \lesssim \varepsilon \qquad (8)$$

for the data used in the analysis. For $\varepsilon \lesssim 1$ stable fits are obtained yielding the Λ value used for the Monte Carlo generation of the data.

The statistical precisions for Λ obtained in the

analysis using different cms-energies, different ranges in x and comparing the results for the full phase space and the range given in fig.1 are summarized in table 1.

Table 1 Statistical precision on Λ and α_s from QCD fits to $\partial\sigma_{NC}(e^+) \approx F_2^{em}$

x-range	type of fit	Λ [MeV]	restricted range Λ [MeV]	α_s	(Q^2) [GeV]
a) $\sqrt{s} = 314$ GeV, $Q^2 \geq 100$ GeV^2, $\int \mathcal{L}\,dt = 200\ pb^{-1}$					
$x \geq 0.25$	non-singlet	145 ± 48	175 ± 176	0.132 ± 0.023	2770
$x \geq 10^{-2}$	" + singlet	297 ± 76	177 ± 135	0.159 ± 0.026	400
$x \geq 10^{-2}$	" + singlet, $xG(x,Q_0^2)$ fixed	215 ± 16	201 ± 25	0.164 ± 0.005	400
b) $\sqrt{s} = 314$ GeV, $Q^2 \geq 10$ GeV^2, $\int \mathcal{L}\,dt = 100\ pb^{-1}$					
$x \geq 10^{-4}$	non-singlet + singlet	196 ± 5	225 ± 25	0.204 ± 0.006	80
c) $\sqrt{s} = 134$ GeV, $Q^2 \geq 18$ GeV^2, $\int \mathcal{L}\,dt = 100\ pb^{-1}$					
$x \geq 0.25$	non-singlet	200 ± 47	460 ± 263	0.193 ± 0.028	530
$x \geq 10^{-2}$	" + singlet	211 ± 27	227 ± 58	0.188 ± 0.012	160

Using the range fig.1 for $x > 10^{-2}$ and $L = 200\ pb^{-1}$ the error for Λ amounts $\delta\Lambda \sim 140$ MeV. This can be improved further using constraints on xG from other measurements and including data at lower y. The extension of the kinematical range to lower x would yield a significant improvement. In the analysis [5] only the leading-log Altarelli-Parisi evolution was considered. For this case a precision $\delta\Lambda \sim 25$ MeV is estimated for $x > 10^{-4}$ and $L = 100\ pb^{-1}$. Since new dynamical effects are expected to influence the data at very low x [6-8] the analysis of the low-x HERA data requires the inclusion of these effects which has not yet been considered. For a low-energy option at HERA with $\sqrt{s} = 134$ GeV the precision of Λ is estimated by $\delta\Lambda \sim 60$ MeV for $x > 10^{-2}$ and $L =$

100 pb^{-1}. Pure non-singlet fits of F_2, i.e. for $F_2^{val} \simeq F_2$ at $x>0.25$ yield rather large errors even for L=200 pb^{-1} since most of the data are located at smaller x.

A major systematical effect in the measurement of Λ are systematic shifts of the cross section due to miscalibrations of the hadronic and electromagnetic calorimeters, cf. section 2. To illustrate this we considered 1% shifts in the measured hadronic or electromagnetic energy E_H and E_e resp. For $Q^2 > 100$ GeV^2, $x > 10^{-2}$ and $\delta E_H/E_H = \pm .01$ $\Delta\Lambda = \pm 70$ MeV is obtained. Since $\delta E_H/E_H$ is expected to be of 2 % this error is of the size of the statistical error for L=200 pb^{-1}. For $Q^2 <$ 100 GeV^2, $10^{-4} < x < 10^{-2}$ and $\delta E_e/E_e = \pm .01$ one finds $\Delta\Lambda = \mp 40$ MeV which also is comparable to the according statistical error.

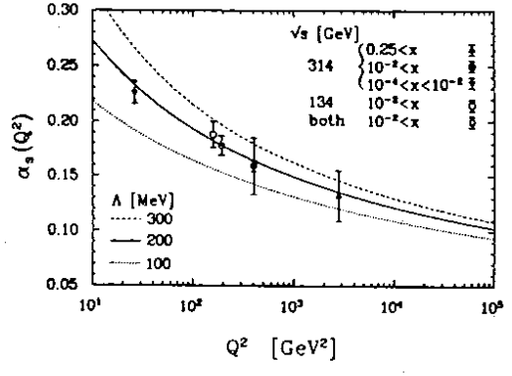

Fig. 10: Statistical precision of the Q^2 dependence of $\alpha_s(Q^2)$

In fig. 10 different measurements for Λ (cf. table 1) are represented in terms of $\alpha_s(Q^2)$ using measurements at the two beam energies $\sqrt{s}$ = 134 GeV (L=100 pb^{-1}) and 314 GeV (L=200 pb^{-1}) and different ranges of x. The inner error bars correspond to the case were the gluon distribution is assumed to be known completely. A variation of $\alpha_s(\langle Q^2 \rangle)$ can be seen comparing the values at high and low Q^2. Together with measurements at intermediate values of Q^2, this could give evidence for the running of the strong coupling.

6. The Gluon Distribution

For many processes in $p\bar{p}$-collisions at high s the detailed knowledge of the gluon distribution at small x is required. HERA offers different possibilities to measure or to constrain this distribution at small x in different ranges of Q^2.

From the simultaneous solution of the Altarelli-Parisi evolution equations of F_2 and xG the gluon distribution can be measured at a given Q_o^2. The statistical precision of this measurement was estimated in [4] using the range $x > 10^{-3}$ and $Q^2 > 10$ GeV^2. In fig.11 a 1σ error contours are given for $xG(x,Q_o^2)$ [23], Q_o^2= 4 GeV fixing Λ = 200 MeV. The hatched range corresponds to the sta-

tistical error using an integrated luminosity of L=100pb^{-1} the dotted line illustrates the effect of additional overall systematic errors of 2 % . Results on a joint fit of $xG(x,Q_0^2)$ and Λ are shown in fig.11 b for different input distributions: xG(DO) and $0.3\times G(DO)/\sqrt{x}$ which can be distinguished clearly in the low x range.

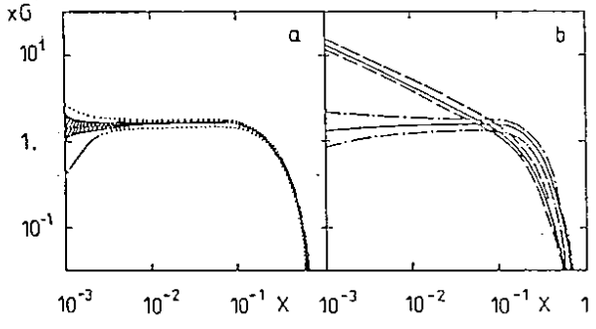

Fig. 11 Extraction of $xG(x,Q_0^2)$ in a QCD analysis for $x > 10^{-3}$

Due to the simplicity of the splitting functions P_{qq}^L and P_{qg}^L for the longitudinal structure function for γ-exchange an approximate representation for $xG(x,Q^2)$ can be obtained [11] at low x.

$$xG(x,Q^2) \approx \frac{3}{5} 5.9 \left[\frac{3\pi}{4\alpha_s} F_L(0.4x,Q^2) - \frac{1}{2} F_2(0.8x,Q^2) \right] \quad (9)$$

To measure xG(x) at x a measurement of F_L at 0.4 x and of F_2 at 2*0.4x is required. As lined out in [11] xG can be determined in the range $Q^2 \sim 50...100$ GeV^2 for $x \sim 0.003...0.02$. In fig. 11 two estimates are given on the precision to measure xG using (9) . The statistical

errors correspond to L = 100 pb^{-1}. Again the input distributions $xG(x,Q_0^2) \sim$ const. and $xG(x,Q_0^2) \sim 1/\sqrt{x}$ can be distinguished for $x \to 0$.

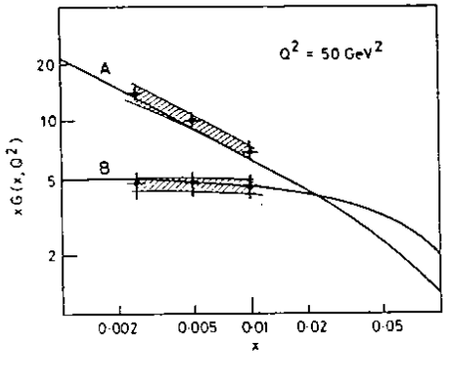

Fig.12 Determination of $xG(x,Q^2)$ from $F_L(x,Q^2)$ and $F_2(x,Q^2)$

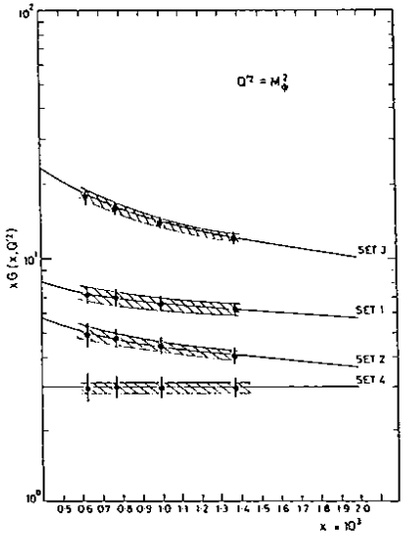

Fig.13: Determination of $xG(x,M_\psi^2)$ from $d\sigma/dy(\gamma g \to J/\psi x)$

The gluon distribution can be measured from the of the production cross section $\gamma g \longrightarrow J/\psi X$ also [12]. In this process Q^2 is fixed by $Q^2 \sim M_\psi^2$. The y dependence of the cross section is given by

$$\frac{d\sigma}{dy} = 1.5 \frac{\alpha}{\pi} \frac{1+(1-y)^2}{y} \bar{x} G(\bar{x},M_\psi^2) \ln \frac{Q^2_{max}}{Q^2_{min}} nb \quad (10)$$

with $\bar{x} \approx 1.5$ x. Estimates on the precision $xG(x,M_\psi^2)$ using different parametrizations (SET 1-3 [24] and SET 4: $xG(x) = 3(1-x)^5$) are illustrated in fig. 13 [12]. The statistical

errors correspond to L=100pb^{-1} and the error due to overall normalization.

As discussed in [13] also cross section measurements of open charm production $e^{\pm}p \to e^{\pm} c\bar{c}$ X can be used to constrain the gluon distributions. To apply this method detailed Monte Carlo studies are required to simulate the background reactions correctly.

7. Conclusions

Structure function measurements at HERA will extend the kinematic range of present day lepton scattering experiments up to $Q^2 \sim$ few 10^4 GeV^2 and down to $x \sim 10^{-4}$. The first time charged current reactions will be measured in $e^{\pm}$ p-scattering at a statistics of a few 10^3 events. Aside the measurement of the kinematical variables from the scattered electron their measurement from the current jet becomes rather important to control systematic effects.

The $O(\alpha)$ electroweak radiative corrections to deep inelastic neutral and charged current reactions are well understood now [16-21] and are controlled at the per cent level.

Among the various structure functions and combinations of parton distributions to be measured only $F_2(x,Q^2)$ can be determined with sufficient precision both

in x and Q^2 [9]. Other distributions can be measured as shapes in x by unfolding from four measured cross sections $\hat{\sigma}^{\pm}_{NC}$, $\hat{\sigma}^{\pm}_{CC}$ or approximations of combinations of them which are valid in certain kinematical ranges [9,10].

Different ways exist to measure or to constrain the gluon distribution [4,11-13], particularly at small x. Statistically one can distinguish the behaviour $xG(x,Q^2) \sim$ const. and $xG(x,Q^2) \sim 1/\sqrt{x}$.

The structure function $F_2(x,Q^2)$ can be precisely measured up to very low x and could be a frist testing ground for new contributions influencing the evolution and shape of F_2 at low x [6-8].

The statistical precision on Λ for $\sqrt{s}$ = 314 GeV, $x > 10^{-2}$, $y > .03$, L = 200 pb^{-1} is $\sim$100 MeV. It could be improved by: i) using constraints on $xG(x,Q^2)$ from other measurements in the analysis, ii) including data at lower y, $y \sim 0.01$, iii) running also at lower $\sqrt{s} \simeq$ 134 GeV, iv) extending the analysis down to $x = 10^{-3} \ldots 10^{-4}$. It is effected by miscalibrations of the electromagnetic and hadronic calorimeters.

All measurements of the above quantities are long term tasks and require the control of the systematics at the per cent level.

References

[1] ZEUS Collaboration, Technical proposal, DESY,1986; H1 Collaboration, Technical proposal, DESY,1986.

[2] HERA - a proposal for a large electron-proton colliding beam facility, DESY/HERA 81/10 (1981).

[3] For reviews on deep inelastic scattering experiments,cf.:
F. Eisele, Rep. Progr. Phys. 49 (1986) 233;
M. Diemoz, F. Ferroni, E. Longo, Phys. Rep. 130 (1986) 293;
T. Sloan, G. Smadja, R.Voss, Phys.Rep. 162 (1988) 45.

[4] J. Bluemlein, M. Klein, T. Naumann, Proc 'New Theories in Physics', Kazimierz, Poland, 1988, Eds. Z. Ajduk et al., World Scientific, 1989, p.228.

[5] J. Bluemlein, G.Ingelman, M.Klein, R.Rueckl, Z. Phys. C45(1990)501.

[6] J. Kwiecinski, Z. Phys. C29 (1985) 561.[7] L.V. Gribov, E.M. Levin, M.G. Ryskin, Phys. Rep. 100(1983) 1.

[8] J. Bartels, J. Bluemlein, G. Schuler, in preparation.

[9] J. Bluemlein, M. Klein, T. Naumann, T. Riemannn Proc. of the HERA Workshop, Hamburg 1987, Ed. R.D. Peccei, (DESY Hamburg,1988) Vol.1, p.67.

[10] G. Ingelman, R.Rueckl, Phys. Lett.B 201 (1988) 369; Z.Phys. C44 (1989) 291.

[11] A.M. Cooper-Sarkar, G. Ingelman, K.R. Long, R. G. Roberts, D.H. Saxon, Z. Phys. C39 (1988) 281.

[12] S.M. Tkaczyk, W.J. Stirling, D.H. Saxon, Proc. of the HERA Workshop, Hamburg 1987, Ed. R.D. Peccei, (DESY Hamburg,1988) Vol.1, p.265; A.D.Martin, C.K.Ng and W.J.Stirling, Phys.Lett. B191 (1987) 200.

[13] G.Barbagli, G.D'Agostini, Proc.of the HERA Workshop, Hamburg 1987, Ed. R.D.Peccei, (DESY Hamburg, 1988), Vol.1, p.135.

[14] J. Feltesse, Proc. of the HERA Workshop, Hamburg 1987, Ed. R.D.Peccei, (DESY Hamburg,1988) Vol.1, p.33.

[15] R. Brinkmann, F. Willeke, private communication.

[16] M. Boehm, H. Spiesberger, Nucl. Phys. B294(1987) 1081;B303(1988) 749.

[17] D. Y. Bardin, C. Burdik, P.C. Christova, T. Riemann, Z. Phys. C42 (1989) 679; C44 (1989) 149.

[18] W. Beenakker, F. A. Berends, W.L. van Neerven, Proc. 'Radiative corrections for e e collisions' , Ringberg, Bavaria, 1989, Ed. J.H. Kuehn, (Springer, Berlin, 1989) p.3.

[19] J. Bluemlein, Berlin preprint PHE 89-08;89-12 and Z. Phys. C in press.

[20] H. Spiesberger, in preparation.

[21] J. Bluemlein, Berlin preprint PHE 90-06.

[22] W. Furmanski, R. Pretronzio, Nuck. Phys. B195 (1982) 237;
L.F. Abbott, W.B. Atwood, R.M. Barnett, Phys. Rev. D22 (1982) 582.

[23] D.W. Duke, J.F. Owens, Phys. Rev. D30 (1984) 49.

[24] A.D.Martin, R.G.Roberts, W.J.Stirling, Phys.Rev. D37 (1988) 1161.

+) Contribution to the Proceedings of the Workshop on Hadron Structure Functions and Parton Distributions, FERMILAB, April, 1990